

Birefringence of SrTiO<sub>3</sub> Produced by the 105°K Structural Phase Transition

Eric Courtens

IBM Zurich Research Laboratory, 8803 Rüschlikon, Switzerland

(Received 11 May 1972; revised manuscript received 25 September 1972)

Accurate birefringence measurements on monodomain SrTiO<sub>3</sub> platelets give important information about the fluctuations associated with the second-order structural phase transition. Above the transition, the monodomain character is announced by a birefringence tail caused by anisotropic fluctuations. Because of these, a distinct cusp is observed at the transition temperature  $T_a$ . Below  $T_a$ , the difference  $\langle \varphi_c^2 \rangle - \langle \varphi_a^2 \rangle$  between mean-square rotations  $\varphi_c$  associated with the order parameter and orthogonal rotations  $\varphi_a$  is obtained.

Structural phase transitions have been the subject of many recent investigations.<sup>1</sup> This is particularly true of the cubic-to-tetragonal transition in SrTiO<sub>3</sub> associated with alternate rotations  $\varphi_c \exp(-i\vec{q}_R \cdot \vec{R})$  of the TiO<sub>6</sub> octahedra around their fourfold axes,  $\langle \varphi_c \rangle$  being the (generalized) order parameter. Much static<sup>2</sup> and dynamic<sup>3</sup> information has already been obtained on this system, and evidence for an extended critical region presented.<sup>4</sup> This Letter reports on accurate birefringence measurements performed on a monodomain platelet.<sup>5</sup> The birefringence is related to the order parameter<sup>6</sup> and is sensitive to fluctuations.<sup>7</sup> Above and at  $T_a$  it shows the fluctuation anisotropy caused by the orienting mechanism producing the monodomain character. Below the transition it essentially probes the difference  $\langle \varphi_c^2 \rangle - \langle \varphi_a^2 \rangle$  of squares of local rotation angles around and perpendicular to the  $c$  axis.

A thin (110) platelet of dimensions  $\sim 7 \times 2 \times 0.27$  mm, with its longer side parallel to [001], was used for the measurement. From previous EPR results it is known that such platelets become nearly monodomain below  $T_a$ , with the  $c$  axis along [001].<sup>5</sup> The use of a monodomain sample is essential to achieve accuracy and reproducibility. A 1-mW 6328-Å laser probed a central region of  $\sim \frac{1}{2}$  mm diam. A Berek compensator well suited for small retardations was employed,<sup>8</sup> and was followed by an analyzer and photomultiplier. The compensation curve, obtained by rotating the compensator plate around the [001] direction, was recorded digitally and fitted by least squares with the theoretical response. A retardation accuracy of  $\pm 2 \times 10^{-4} \lambda$  was achieved for compensator retardations  $\Gamma_c < 2 \times 10^{-2} \lambda$ , beyond which the error increased linearly with  $\Gamma_c$ . The sample was placed in a temperature-controlled enclosure mounted in a cold-finger optical cryostat. In the region of  $T_a$  the temperature stability was esti-

mated to be better than 0.01°C, with a relative reading accuracy of  $\pm 0.02^\circ\text{C}$ .

The general behavior of  $\Delta n$  for  $T < T_a$  is shown in Fig. 1. The zero of the data points has been displaced vertically; the actual zero of  $\Delta n$  occurred around 98.5°K in all the measurements presented here. To achieve the highest measuring accuracy in the region of  $T_a$ , the compensator plate was usually given a constant, slight tilt (rotation around [110]), which compensated the negative birefringence background. The present results are in agreement with previous observations.<sup>9</sup> It seems logical to associate the constant negative background observed far above  $T_a$  to the orienting mechanism causing the monodomain character below  $T_a$ . This mechanism could be built-in strains, or also a very slight distortion

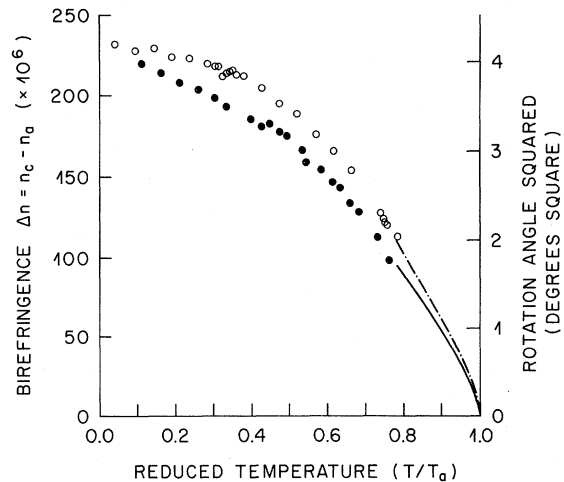


FIG. 1. Closed circles, low-temperature birefringence data extrapolated by the solid line which is the fit of Fig. 2(a). Open circles, square of the order parameter measured on Fe<sup>3+</sup> centers (Ref. 15), extrapolated by the dash-dotted line which is the fit of Ref. 4. The  $\Delta n$  and  $\langle \varphi_c \rangle^2$  scales correspond as explained in the text.

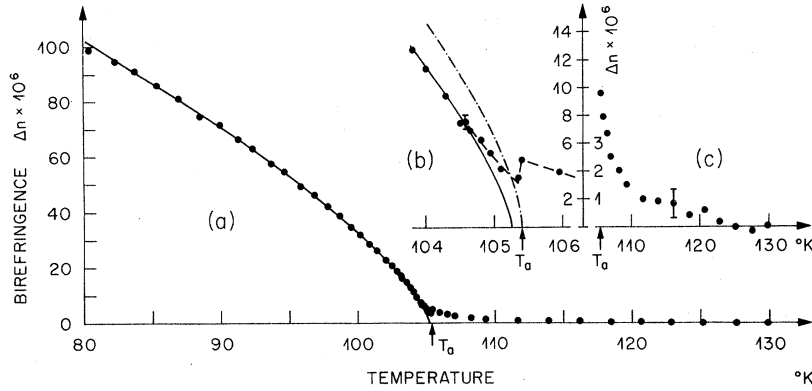


FIG. 2. Birefringence data around  $T_a$ . Solid line, exponential fit explained in the text. (a) Entire temperature range; (b) exact vicinity of  $T_a$  on a greatly expanded scale. The cusp position is shown by the arrow. The dash-dotted line is a properly scaled replica of  $\langle \varphi_c \rangle^2$  from Ref. 4. The dashed line passes through the experimental points. (c) Birefringence tail expanded vertically.

of the cubic phase which might exist above  $T_a$ .<sup>10</sup> In either case the constant background can be subtracted, giving curves which represent the effect of the softening of the  $\tilde{q}_R$  optical phonon on the birefringence. The region of  $T_a$  is shown in detail in Fig. 2, where the cusp [Fig. 2(b)], and the tail [Fig. 2(c)] are presented on appropriately expanded scales.

Let the light propagate in the  $-\hat{x}$  direction, with its polarization vector bisecting  $\hat{y}$  and  $\hat{z}$ , in a slab parallel to the  $yz$  plane and of thickness  $L$ . The compensator, of variable retardation  $\Gamma_c$ , has its main vibration directions parallel to  $\hat{y}$  and  $\hat{z}$ . The inverse optical dielectric tensor of the medium  $\epsilon_{\alpha\beta}^{-1} = \epsilon_0^{-1} \delta_{\alpha\beta} + \Delta\epsilon_{\alpha\beta}^{-1}$  is composed of a large constant isotropic part and of a small space-time-dependent anisotropy  $\Delta\epsilon_{\alpha\beta}^{-1}$  (Greek subscripts refer to  $x$ ,  $y$ , and  $z$ ). An eikonal approach<sup>11</sup> can be used, provided that the gradient of the fluctuations in the inverse dielectric tensor is much smaller than  $2\pi/\lambda n_0$ , where  $\lambda$  is the vacuum wavelength and  $n_0 = \sqrt{\epsilon_0}$ . My results indicate that this holds for SrTiO<sub>3</sub>, even for large fluctuations whose size would be as small as the unit cell. For small anisotropies the difference between wave normal and ray directions is negligible; one must only account for local fluctuations of the main vibration directions in the  $yz$  plane. The light sees the fluctuations as *static* provided the slowing down relaxation time is longer than both the optical period and the flight time over a correlation length, which is well satisfied for

SrTiO<sub>3</sub>. For retardations much smaller than a quarter wave, the average intensity detected after the analyzer is then<sup>12</sup>

$$I = I_0 (\pi^2/\lambda^2) [(\langle \Gamma_s \rangle - \Gamma_c)^2 + B], \quad (1)$$

where  $I_0$  is the incident intensity, and  $\Gamma_s = (\Delta\epsilon_{yy}^{-1} - \Delta\epsilon_{zz}^{-1})Ln_0^3/2$ . Angular brackets denote ensemble averaging. By varying  $\Gamma_c$  the compensation curve is obtained, from which  $\langle \Gamma_s \rangle$  is deduced. The plotted quantity is  $\Delta n = \langle n_z - n_y \rangle = \langle \Gamma_s \rangle/L$ . The background is

$$B = \langle \int \delta\Gamma_s(x, y, z, t) \delta\Gamma_s(x + \xi, y, z, t) d\xi \rangle_{y,z,t} / L,$$

where  $\delta\Gamma_s = \Gamma_s - \langle \Gamma_s \rangle$  is a totally depolarized contribution which would in principle allow a measurement of higher-order correlations. In SrTiO<sub>3</sub>,  $\Delta n$  being itself very small, the background was too small to be reliably measured.

Using these considerations, the results on SrTiO<sub>3</sub> can be interpreted in terms of current theories by allowing the phase-transition contribution to  $\overline{\epsilon}^{-1}$  to be expanded as a function of the *local* rotation angles  $\varphi_i$  (Latin subscripts refer to crystal axes  $a$ ,  $a'$ , and  $c$ ). One writes  $\Delta\epsilon_{ij}^{-1} = T_{ijkl}\varphi_k\varphi_l$ , where  $T$  is a fourth-order cubic tensor. The orienting mechanism affects  $\overline{\epsilon}^{-1}$  in two ways: first, through its effect on the  $\varphi_i$ 's; second, by the background contribution (though the strain-optic tensor, in the case of strain) already subtracted by the ordinate shift. For the present sample orientation one obtains

$$\Delta n = n_0^3 \left[ \frac{1}{2}(T_{1122} - T_{1111})(\langle \varphi_c^2 \rangle - \frac{1}{2}\langle \varphi_a^2 \rangle - \frac{1}{2}\langle \varphi_{a'}^2 \rangle) - T_{1212}\langle \varphi_a \varphi_{a'} \rangle \right]. \quad (2)$$

From symmetry considerations  $\langle \varphi_a^2 \rangle = \langle \varphi_{a'}^2 \rangle$ . The tetragonal symmetry below  $T_a$  (neglecting a pos-

sibly lower symmetry due to the orienting mechanism) leads to  $\langle \varphi_a \varphi_a' \rangle = 0$ . The major portion of  $\Delta n$  below  $T_a$  is then

$$\Delta n = S(\langle \varphi_c \rangle^2 + \langle \delta \varphi_c^2 \rangle - \langle \varphi_a^2 \rangle), \quad (3)$$

where  $\delta \rho_c \equiv \varphi_c - \langle \varphi_c \rangle$  (whereas  $\langle \varphi_a \rangle = 0$ ) and  $S = n_0^3(T_{1122} - T_{1111})/2$ . The birefringence behavior differs from the square of the order parameter, also shown in Fig. 1, by the fluctuation difference  $\Delta \equiv \langle \delta \varphi_c^2 \rangle - \langle \varphi_a^2 \rangle$ . This quantity plays an important role in microscopic theories of the transition, but its critical behavior is not known outside mean-field theory.<sup>13</sup> By neglecting the contribution of the orienting mechanism,  $\Delta$  should be negative below  $T_a$  since the curvature of the potential well is higher in the  $\varphi_c$  than in the  $\varphi_a$  direction or, similarly, since the frequency of the doubly degenerate soft mode is lower than that of the singly degenerate one. Below  $\sim 30^\circ\text{K}$ , changes in  $\Delta$  are entirely controlled by the decrease of  $\langle \varphi_a^2 \rangle$  with  $T$  proportional to  $(\hbar\omega_2)^{-1} \coth(\hbar\omega_2/2kT)$ , where  $\omega_2$  is a frequency of the order of the lowest optic branch frequency ( $\sim 2$  meV).<sup>14</sup> This quantity varies as  $\coth(12^\circ\text{K}/T)$ , which accounts for the nearly linear increase of  $\Delta n$  at very low temperatures. A fit of this sort also leads to an estimate of  $\langle \varphi_a^2 \rangle_0$ , the zero-point fluctuations, found to be very small. Since  $\langle \delta \varphi_c^2 \rangle_0 < \langle \varphi_a^2 \rangle_0$  on theoretical grounds, the  $\langle \varphi_c \rangle^2$  curve obtained by EPR<sup>15</sup> can be scaled to  $\Delta n$  such that the two curves almost meet at  $0^\circ\text{K}$  (Fig. 1). The ordinate difference of these curves is roughly equal to  $\Delta$ , negative throughout the low-temperature phase except for the exact vicinity of  $T_a$  [Fig. 2(b)]. From this scaling one obtains  $S \approx 55 \times 10^{-6} \text{ deg}^{-2}$ .

Above and immediately around  $T_a$  [Figs. 2(b)–2(c)], the birefringence is small and governed by the effect on fluctuations of the orienting mechanism. In its absence one would have  $\Delta n = 0$ , for  $T > T_a$ . Rotations around the  $c$  direction being favored by the mechanism, a positive value of  $\Delta$  results, in agreement with the observation. A possible contribution of  $\langle \varphi_a \varphi_a' \rangle$  above  $T_a$  cannot be ruled out, the difficulty being associated with the particular crystal orientation required to obtain a monodomain. A comparison with the EPR linewidth<sup>3</sup> is, however, worthwhile. The EPR shows cusps both in  $\langle \varphi_c^2 \rangle$  and  $\langle \varphi_a^2 \rangle$ , whose difference should be of the order of the birefringence cusp. The EPR linewidth measurement is performed almost entirely in the motional narrowing limit. Only in the close vicinity of  $T_a$  is an inhomogeneous line observed, indicating fluctua-

tions *slower* than the characteristic measuring frequency. This latter regime is that of the birefringence measurement throughout the *entire* temperature range. Therefore, comparison with EPR can only be made at  $T_a$ , where the linewidth results give  $\langle \varphi_c^2 \rangle = 0.107$  and  $\langle \varphi_a^2 \rangle = 0.016 \text{ deg}^2$ . This gives  $\Delta n \approx S(\langle \varphi_c^2 \rangle - \langle \varphi_a^2 \rangle) = 5.0 \times 10^{-6}$ , in remarkable agreement with the peak amplitude in Fig. 2(b). These considerations also show that  $\langle \varphi_c^2 \rangle$  is much larger than  $\langle \varphi_a^2 \rangle$  in the tail. Hence, it is reasonable to attempt a fit of this tail using an integral over  $\vec{q}$  space of an appropriate static structure factor. The result of such a fit<sup>12</sup> lends further support to a strong anisotropy of the structure factor.<sup>3</sup>

Finally, we discuss the critical region below  $T_a$  [Figs. 2(a)–2(b)]. By studying the curvature of the potential well in a Landau model,<sup>16</sup> it is easy to see qualitatively that, whatever the orienting mechanism, it will strongly reduce  $\langle \varphi_a^2 \rangle$  in the region of  $T_a$ , but will have little or no effect on  $\langle \delta \varphi_c^2 \rangle$ , except for a small overall  $T_a$  displacement.  $\Delta$ , positive at  $T_a$ , changes sign as the temperature is reduced. This sign reversal takes place rapidly, within much less than a degree from  $T_a$ , as seen from the EPR linewidth.<sup>3</sup> This is also seen in Fig. 2(b), where  $\langle \varphi_c \rangle^2$  from Ref. 4 is drawn with the scale determined in Fig. 1 and using the value of  $T_a$  given by the cusp position ( $T_a = 105.41^\circ\text{K}$ ). This dash-dotted curve crosses the dashed experimental one around  $T = 105.25^\circ\text{K}$ , where  $\Delta$  changes sign. Because of this complicated behavior, a true exponential fit is not expected to hold up to  $T_a$ . An excellent least-squares fit to the points between  $90$  and  $104.3^\circ\text{K}$  is  $\Delta n = 10^{-5} \times (105.26^\circ\text{K} - T)^{0.72}$ . This is the solid line drawn in Figs. 1 and 2(a)–2(b). The small difference between the origin of this fit and the actual  $T_a$  is probably meaningful, given the temperature reading accuracy. It is another manifestation of the complication caused by the orienting mechanism. Inasmuch as  $\Delta$  is small compared to  $\langle \varphi_c \rangle^2$ , the exponent, whose accuracy is  $\pm 0.02$ , should be of the order of  $2\beta$ . This exponent is definitively smaller than its expected mean-field value of 1.<sup>13</sup>

In conclusion, the birefringence results give valuable information on fluctuations and the anisotropy produced by the orienting mechanism. In multidomain crystals such anisotropy also seems to exist within individual domains, and in fact appears to have a fairly constant effect on EPR resonance lines.<sup>17</sup> Since no measurement can claim to be free of it, a better understanding

of this mechanism will certainly improve the description of the transition.

The author is grateful to Hansjörg Kaehr for his able technical assistance. He is much indebted to K. A. Müller for stimulating discussions, comments on the manuscript, and the communication of unpublished results. He has also benefitted from conversation with H. Thomas, T. Schneider, Th. von Waldkirch, and W. Berlinger, as well as from valuable suggestions of H. Gränicher and K. W. Blazey.

<sup>1</sup>*Structural Phase Transitions and Soft Modes*, edited by E. J. Samuelsen and J. Feder (Universitetsforlaget, Oslo, Norway, 1971).

<sup>2</sup>See Ref. 1 and references quoted therein.

<sup>3</sup>Th. von Waldkirch, K. A. Müller, W. Berlinger, and H. Thomas, *Phys. Rev. Lett.* **28**, 503 (1972); Th. von Waldkirch, K. A. Müller, and W. Berlinger, *Phys. Rev. B* (to be published).

<sup>4</sup>K. A. Müller and W. Berlinger, *Phys. Rev. Lett.* **26**, 13 (1971).

<sup>5</sup>K. A. Müller, W. Berlinger, M. Capizzi, and H. Gränicher, *Solid State Commun.* **8**, 549 (1970). The author is very grateful to K. A. Müller and W. Berlinger for the loan of the sample used in Ref. 4. The curves reported here were obtained on the same crystal.

<sup>6</sup>This relation is experimentally known in other systems. See, for example, G. Egert, I. R. Jahn, and

D. Renz, *Solid State Commun.* **9**, 775 (1971).

<sup>7</sup>The effect of fluctuations on optical properties has been seen in the case of the paraelectric-ferroelectric transition. See, for example, R. Hofmann, Ph. D. thesis, Eidgenössische Technische Hochschule, 1968 (unpublished); M. G. Cohen, M. Di Domenico, Jr., and S. H. Wemple, *Phys. Rev. B* **1**, 4334 (1970).

<sup>8</sup>M. Born and E. Wolf, *Principles of Optics* (Pergamon, New York, 1965), 3rd ed., p. 694. The author is indebted to Professor H. Gränicher for suggesting this compensator and for loaning an instrument at the beginning of the investigation.

<sup>9</sup>L. E. Cross and D. Chakravorty, in *Proceedings of the International Meeting on Ferroelectricity, Prague, Czechoslovakia, 1966*, edited by V. Dvořák *et al.* (Institute of Physics of the Czechoslovak Academy of Science, Prague, Czechoslovakia, 1966), p. 394.

<sup>10</sup>F. W. Lytle, *J. Appl. Phys.* **35**, 2212 (1964).

<sup>11</sup>M. Born and E. Wolf, *Principles of Optics* (Pergamon, New York, 1965), 3rd ed., pp. 110–112.

<sup>12</sup>Detailed information will be published elsewhere.

<sup>13</sup>E. Pytte and J. Feder, *Phys. Rev.* **187**, 1077 (1969); J. Feder and E. Pytte, *Phys. Rev. B* **1**, 4803 (1970).

<sup>14</sup>J. Feder, in *Structural Phase Transitions and Soft Modes*, edited by E. J. Samuelsen and J. Feder (Universitetsforlaget, Oslo, Norway, 1971).

<sup>15</sup>Experimental data points communicated by K. A. Müller and W. Berlinger.

<sup>16</sup>J. C. Slonczewski and H. Thomas, *Phys. Rev. B* **1**, 3599 (1970).

<sup>17</sup>K. A. Müller, private communication.

## Two-Dimensional Character of the Conduction Bands of *d*-Band Perovskites\*

T. Wolfram

*North American Rockwell Science Center, Thousand Oaks, California 91360*

(Received 14 August 1972)

The lowest conduction bands of a number of perovskites are determined principally by the ( $pd\pi$ ) interaction which mixes the  $t_{2g}$   $d$  orbitals of the transition-metal ion with the  $p$  orbitals of the oxygen. Because of the planar character of the ( $pd\pi$ ) interaction, each of the three equivalent  $t_{2g}$  conduction bands depends strongly on only two of the components of the wave vector. As a result, the bands possess a two-dimensional character which accounts for the characteristic structure in the density of states and the optical properties of SrTiO<sub>3</sub>, BaTiO<sub>3</sub>, and KTaO<sub>3</sub>.

The transition-metal perovskites such as SrTiO<sub>3</sub>, BaTiO<sub>3</sub>, and KTaO<sub>3</sub> have received considerable attention because of their many interesting electronic,<sup>1-6</sup> structural,<sup>7-9</sup> and optical<sup>10-12</sup> properties. Each of the above-mentioned materials is an ionic insulator with a band gap of 3 to 4 eV separating the  $d$  conduction band from the valence band. BaTiO<sub>3</sub> is ferroelectric<sup>13</sup> below the Curie temperature, and doped SrTiO<sub>3</sub> is a superconductor.<sup>14</sup> The photochromic and electrochromic

properties of SrTiO<sub>3</sub> have been discussed recently,<sup>15-19</sup> and the electronic surface states of the  $d$ -band perovskites have also been studied by Wolfram, Kraut, and Morin.<sup>20</sup> Mattheiss has recently reported energy-band studies of these materials.<sup>2</sup>

The purpose of this Letter is to discuss a simple model which illustrates the two-dimensional nature of the lowest conduction bands. Analytical approximations are obtained for the energy bands